

Periodic stratification in the Rhine ROFI in the North Sea

Freshwater influence
Tidal mixing
Periodic stratification
Coastal region

Eaux douces
Mélange de marée
Stratification périodique
Région côtière

John H. SIMPSON^a, Wim G. BOS^b, Florian SCHIRMER^c, Alejandro J. SOUZA^a, Thomas P. RIPPETH^a, Sarah E. JONES^a and David HYDES^d

^a University of Wales Bangor, School of Ocean Sciences, Menai Bridge, Gwynedd, LL59 5RH, UK.

^b Rijkswaterstaat, Tidal Waters Division, Koningskade 4, 2596 AA The Hague, The Netherlands.

^c University of Hamburg, Institut für Meereskunde, Troplowitzstrasse 7, D 2000 Hamburg 54, Germany.

^d Institute of Oceanographic Sciences, Deacon Laboratory, Wormley, Godalming, Surrey GU8 5UB, UK.

Received 7/09/92, in revised form 20/01/93, accepted 27/01/93.

ABSTRACT

The nature of the physical regime in the vicinity of the Rhine ROFI (Region Of Freshwater Influence) has been determined in a series of collaborative observations. Extensive surveys with shipboard CTD/rosette systems have been used to complement time series observations by an array of moorings instrumented with currentmeters, transmissometers and fluorimeters.

The observations reveal a highly variable system in which the influence of the freshwater input from the Rhine extends northeastwards from the source and out to 30 km from the coast. The mean flow within this region is generally parallel to the coast (northeastwards) and with surface speeds, determined by the HF radar, of 15-20 cm.s⁻¹. The residual current at sub-tidal frequencies was strongly correlated with windstress-forcing with a transfer factor of ~ 1 %.

Water column structure exhibits marked periodic variations particularly on semi-diurnal and semi-monthly time scales, the latter highlighted by contrasting post-springs and post-neaps surveys of the ROFI region. Springs tidal stirring was reinforced by strong wind (and wave) mixing which brought about complete vertical homogeneity everywhere except at the Rhine mouth. After the following neaps, and a period of light winds, the water column was observed to have re-stratified over the whole inshore region through the relaxation of the horizontal gradients under gravity and with the influence of rotation as in the model of Ou (1983).

The switching of the water column regime between stratified and mixed conditions was observed to markedly change the coupling between low frequency surface and bottom currents and is also reflected in the suspended sediment variations. Generally high levels of seston throughout the coastal boundary layer in the post-springs period were followed by a dramatic reduction especially in the region which re-stratified. An interesting exception was the combined occurrence of high turbidity and low salinity in surface waters due to the immediate influence of the Rhine outflow near the source.

Oceanologica Acta, 1993. **16**, 1, 23-32.

RÉSUMÉ

Stratification périodique en Mer du Nord dans la zone d'extension des eaux du Rhin

Les caractéristiques physiques de la Mer du Nord ont été étudiées dans la zone d'influence des eaux du Rhin. Les données ont été acquises à l'aide de sondes CTD montées sur rosettes et complétées par des séries chronologiques obtenues sur des mouillages équipés de courantomètres, transmissomètres et fluorimètres.

Les observations révèlent une grande variabilité liée à l'extension de l'eau douce du Rhin vers le nord-est jusqu'à 30 km de la côte. Le flux moyen dans cette région est généralement orienté vers le nord-est parallèlement à la côte, avec des vitesses superficielles, déterminées par radar HF, de l'ordre de 15-20 cm.s⁻¹. Le courant résiduel, aux fréquences inférieures à celle de la marée, est fortement corrélé à la tension du vent, avec un facteur de transfert d'environ 1 %.

La structure de la colonne d'eau montre des variations périodiques prononcées, en particulier aux échelles semi-diurne et semi-mensuelle; cette dernière est soulignée par contraste avec les observations suivant la marée de vives-eaux et celle de mortes-eaux. L'action de la marée de vives-eaux est renforcée par le brassage dû au vent et aux vagues, qui provoque une homogénéisation de la colonne d'eau, sauf à l'embouchure du Rhin. Après la marée de mortes-eaux suivante et une période de vents faibles, la colonne d'eau se trouve à nouveau stratifiée dans toute la région côtière par affaiblissement des gradients horizontaux sous l'effet de la gravité et de la rotation comme dans le modèle de Ou (1983).

L'alternance des conditions de stratification et de brassage a un effet marqué sur le couplage entre les courants de basse fréquence en surface et au fond, et sur la sédimentation des particules en suspension. Les taux de seston observés dans la couche limite côtière sont généralement élevés après la marée de vives-eaux, puis diminuent beaucoup, en particulier dans la région à nouveau stratifiée. Une exception intéressante est constituée par l'apparition conjointe d'une forte turbidité et d'une faible salinité dans les eaux superficielles sous l'effet des eaux du Rhin.

Oceanologica Acta, 1993. 16, 1, 23-32.

INTRODUCTION

Freshwater from river run-off contributes an important input of buoyancy to those parts of the shelf seas adjacent to estuaries. In consequence, these regions, which we have termed ROFI's (Region Of Freshwater Influence), experience a physical regime which is radically different from the other parts of the shelf seas where heating and cooling

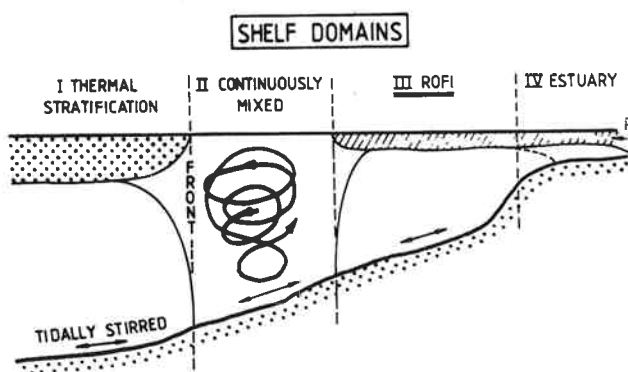


Figure 1

Schematic in the cross-shore direction showing ROFI and other shelf regimes.

through the surface constitute the predominant exchange of buoyancy. Instead of the comparatively regular pattern of seasonal stratification, or complete vertical mixing, determined by heating-stirring competition (*e. g.* Simpson and Bowers, 1984), the typical ROFI system (Fig. 1) experiences alternation between vertically-mixed and stratified conditions in response to the changes in run-off and in the intensity of stirring. The tidal forcing of ROFIs contains regular components in the form of changes in stirring over the spring-neap cycle and the semi-diurnal variation of stirring and straining of the density field (*e. g.* Simpson *et al.*, 1990). At the same time, the variability of run-off and episodes of wind and wave stirring introduce more random components to the variability of the ROFI regime.

The horizontal density gradients maintained by the input of freshwater from the Rhine tend to drive an estuarine circulation in the ROFI. The influence of variable tide and wind stirring, however, makes this flow intermittent as is illustrated in the laboratory experiments of Linden and Simpson (1988). At the scale of the Rhine ROFI, the flow is further complicated by the influence of the earth's rotation which limits the cross-shore movement of the density currents. In a balanced state the cross-shore gradients drive an along-shore flow which forms a classical coastal current flowing from the estuary source with the land on its right (looking

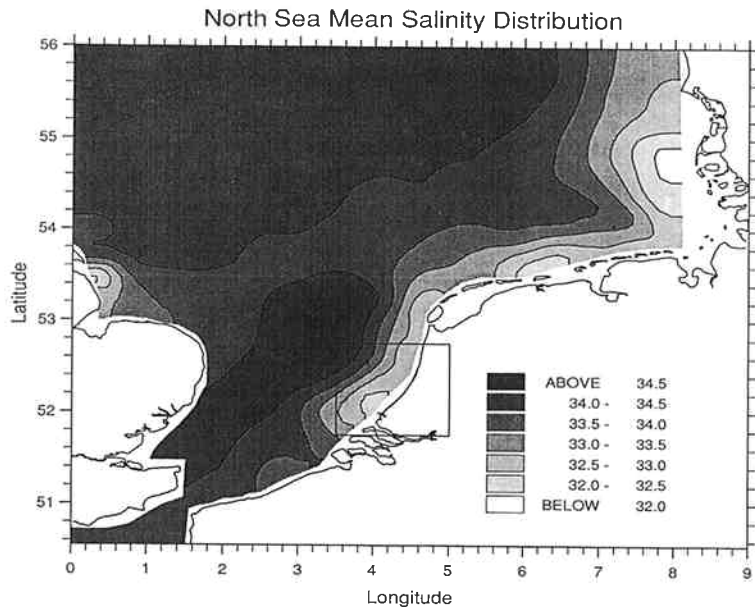


Figure 2

Large scale salinity distribution from North Sea project data between the 27 April and the 9 May 1989.

down current) in the northern hemisphere. A number of such coastal currents have recently been identified and documented (*e. g.* Garvine, 1991)

The interaction between the mean flow of the coastal current and the pattern of vertical structure, evolving in response to the buoyancy stirring competition, presents a substantial challenge to shelf sea physical oceanographers. At the same time, understanding of the ROFI domain is of considerable practical importance in relation to the management of our shelf seas. The pronounced changes in stratification and vertical mixing exert important controls on the vertical flux and distribution of suspended particles and, hence, the optical depth of the water column which in turn influences primary production. The inputs of freshwater from estuaries also frequently bring with them large quantities of land-derived nutrients and contaminants which make their first and, often most severe, impact in the ROFI system.

The discharge of freshwater by the Rhine into the North Sea, at an average rate of $2200 \text{ m}^3 \text{ s}^{-1}$, creates a major ROFI which extends along the Dutch coast and into the German Bight where there are other large freshwater inputs from the estuaries of the Weser and the Elbe. The area of significant salinity deficit (Fig. 2) continues in the direction of the coastal current flow along the Danish coast into the Skaggeiak where it joins the Baltic outflow. The Rhine buoyancy input alone is at a rate of $\sim 5.4 \times 10^5 \text{ N s}^{-1}$ equivalent to peak summer heating over an area of 10^4 km^2 .

The Rhine ROFI has been studied for some years by Dutch scientists, partly because of the need to set up an appropriate coastal zone management. An early insight into the spreading of the outflow was based on quasi-synoptic salinity distributions (*e. g.* van Alphen *et al.*, 1988). More recently De Ruijter *et al.* (1992) have shown that the density field is mainly haline controlled and that the cross-shore density gradient, as observed during several surveys, is related to the along-shore geostrophic flow and the cross-shore estuarine circulation. Above this, in the surface layer, the wind enhances or counteracts the current flow.

Long-term residual currents from one year current meter observations in the Noordwijk transect show a northward coast-parallel current near the surface and an onshore flow at the bottom (Van der Giessen *et al.*, 1990).

The investigation reported here is the first of a series of European collaborative efforts to study the important near-source region of the Rhine ROFI which has been identified as a possible source of "nuisance blooms" driven by the high nutrient content of the Rhine water. It builds on previous studies of the outflow mainly by Dutch oceanographers (*e. g.* van Alphen *et al.*, 1988) which indicate the short time scale of water column stability in the region.

The aim of the surveys was to provide a data base to elucidate the development of structure and flow on time-scales from one hour to one month and allow the testing of models of the ROFI regime. The observational strategy was based on a combination of time-series measurements from a mooring array and HF radar together with quasi-synoptic ship surveys. The extensive ship coverage also provided the opportunity to survey nutrient concentrations and suspended particles.

THE OBSERVATIONS

An extensive programme of measurements was undertaken during September and October 1990 from the research vessels RRS Challenger and the MS Holland. Two arrays of moorings (Fig. 3) were deployed: one cross-shore to observe the transverse section of the alongshore flow field and a diamond array which was designed to determine the structure of the water column and flow and to measure the horizontal gradient of density which forms an important part of the dynamical forcing. Each of the moorings in the central diamond (A-D) was equipped with three currentmeters, the majority of which also recorded temperature and salinity, and a surface TS recorder attached to the toroidal marker buoy. In addition, four recording transmissometers and two fluorometers were deployed at the surface on moorings A

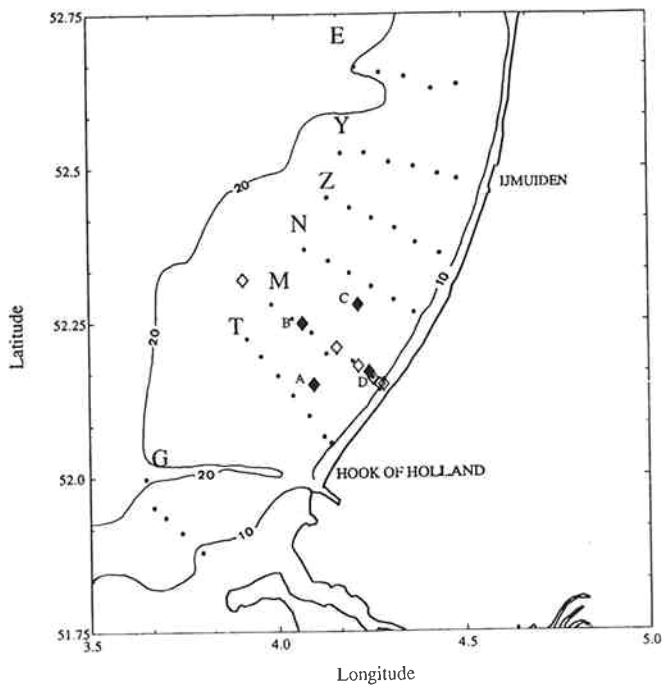


Figure 3

Dutch coast with topography in metres. The dots represent stations and the diamonds the moorings positions (filled diamonds UCNW moorings, blank diamonds RWS moorings).

and C; a fifth transmissometer was located near the sea-bed at mooring A for part of the deployment.

This diamond array was maintained in position from 23 September to 18 October 1990 though one mooring (C) had to be re-positioned to accommodate a major geophysical survey which passed through the area (with official approval from the same maritime authorities that authorised our own survey!).

The Challenger made two spatial surveys of a large sector of the ROFI on the grid of stations shown in Figure 3. The timing of these surveys was chosen to coincide with the post-springs and post-neaps periods to provide the maximum contrast in tidal stirring. Profiles of temperature, salinity, optical beam transmittance and chlorophyll fluorescence were recorded at each station using a NBIS Mk 3 CTD system equipped with auxiliary sensors. Water samples were obtained from selected depths for the determination of nutrients, heavy metals, halocarbon analysis and suspended particulate matter.

In plotting horizontal distributions (*see* Fig. 5, 7, 8), a first order correction for tidal displacement has been applied so that results are plotted at positions corresponding to their location at local high water.

The MS Holland conducted surveys from the outflow region to about 40 km to the north. By limiting the survey area, the Holland was able to obtain more detailed observations of the near outflow region.

For sixteen days during the study period, surface currents were observed over part of the ROFI using the IfM Codar HF radar system. Shore stations, located at Gravensande and Noordwijk, gave coverage out to ~ 40 km, equivalent to a grid of more than 100 current meters spaced at intervals of ~ 3 km.

RESULTS

Time series

The principal parameters observed at mooring A are shown in Figure 4. The predicted cycle of tidal stirring, evident in the tidal current (Fig. 4 a), was augmented by wind-stress (Fig. 4 b) which acted to re-inforce vertical mixing during the central springs period (days 277-281) in contrast to the neaps periods, before and after, when wind stirring was slight. These large changes in mixing are reflected in the water column stratification as seen in the bottom-surface salinity difference (Fig. 4 c). Episodes of strong stratification ($\Delta s > 5$), occurring during the neaps period centred on day 271, are followed by an eight-day period of negligible stratification when strong stirring prevailed. Subsequently, with the approach of neaps and a reduction in windstress, the water column re-stratified and remained stable for several days but with large semi-diurnal oscillations. This pattern of variation, which was also characteristic of the earlier neaps period, represents the combined effects of tidal advection, stirring and straining on the water column.

In tidal straining (*e. g.* Simpson *et al.*, 1990), the vertical shear of the current interacts with the horizontal density gradient to generate stratification during the ebb cycle of the current which is cancelled by reverse shear during the

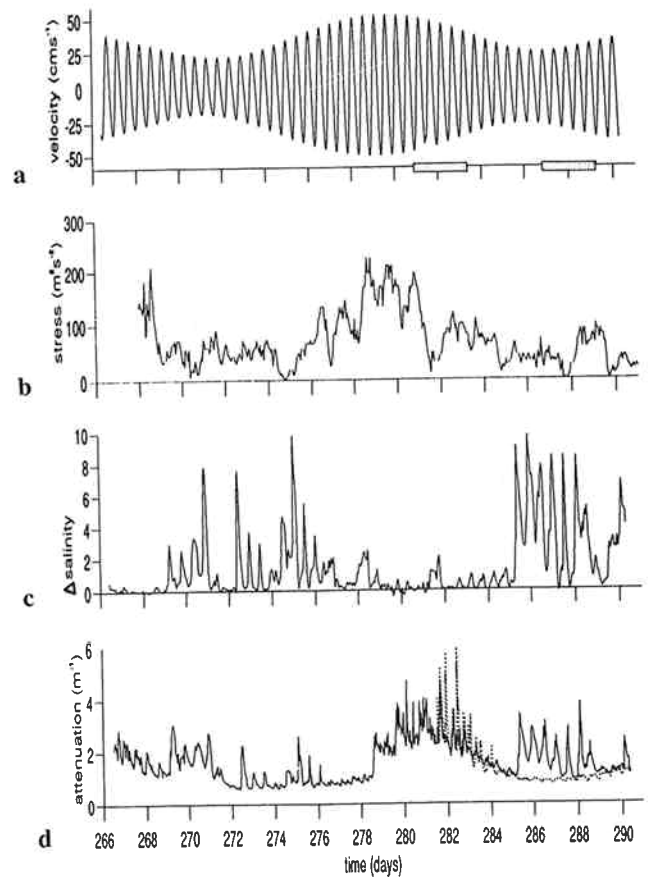


Figure 4

Mooring A time series: a) east-west tidal currents 4 m above the bed; b) windstress magnitude from the Hook of Holland; c) salinity difference between 1 and 16 m below the surface; d) transmittance black line (1 m), dotted line (16 m).

flood. The effect is to produce semi-diurnal variations in stability. In this case, the straining effects may be augmented by the advection of a more stratified water column from near the Rhine source by the oscillating tidal flow.

Optical attenuation c (Fig. 4 b) also exhibited marked temporal variability and a clear correlation with the stirring inputs. Surface optical attenuation declined from the initial spring tide (day 265) towards the subsequent neap with the minimum value ($c = 0.8 \text{ m}^{-1}$) lagging the tidal forcing by two-three days; it increased steeply again after day 278 in response to increasing tidal stirring augmented by strong winds stirring. Thereafter it declined as bottom resuspension diminished. Comparison of surface and near-bottom values of optical attenuation (the latter obtained only from day 281) indicates that the bottom water was more turbid than the surface water immediately after maximum springs (due to tidal stirring). However, this was markedly reversed towards the subsequent neap period: reduced stirring inhibited bottom resuspension so that bottom optical attenuation fell dramatically (c reaching a minimum of 0.8 m^{-1}) while surface c values closely follow Δs with a succession of marked semi-diurnal peaks. Clearly at this time pulses of turbid, low salinity water from the Rhine were passing through the mooring position, generating a periodic turbidity signal (days 285-289) which diminishes towards the end of the record.

Spatial surveys of water column structure

Complementary evidence of the changes in water column structure and the concentration of suspended particles is provided by the contrast between the post-springs and post-neaps spatial surveys. To illustrate the change in stratification between the two situations, we present in Figure 5 the observed distributions of the potential energy anomaly ϕ which represents the amount of work required per unit volume to bring about complete vertical mixing. ϕ is defined as:

$$\phi = \frac{1}{h} \int_{-h}^0 (\bar{\rho} - \rho) g z dz; \quad \bar{\rho} = \frac{1}{h} \int_{-h}^0 \rho dz$$

where $\rho(z)$ is the density profile and h = water column depth.

Figure 5 a represents the situation after springs (days 281-283) when the water column was almost completely mixed over practically the whole survey area. Only in the immediate vicinity of the Rhine source is any significant stratification observed. Six days later, the post-neaps survey (Fig. 5 b) shows strong stratification, with ϕ up to 20 Jm^{-3} , extending out to 30 km from the coast and northwards from the Rhine source to the limit of the survey area.

Spatial structure within the stratified region should, however, be interpreted with caution because of the short term variability. If the rapid semi-diurnal changes in stratification observed at the mooring position are representative of the area, then we should expect severe variability in the apparent spatial distribution of ϕ . At the same time, the duration of the surveys (two-three days) means that the data will not be synoptic because of the evolution of struc-

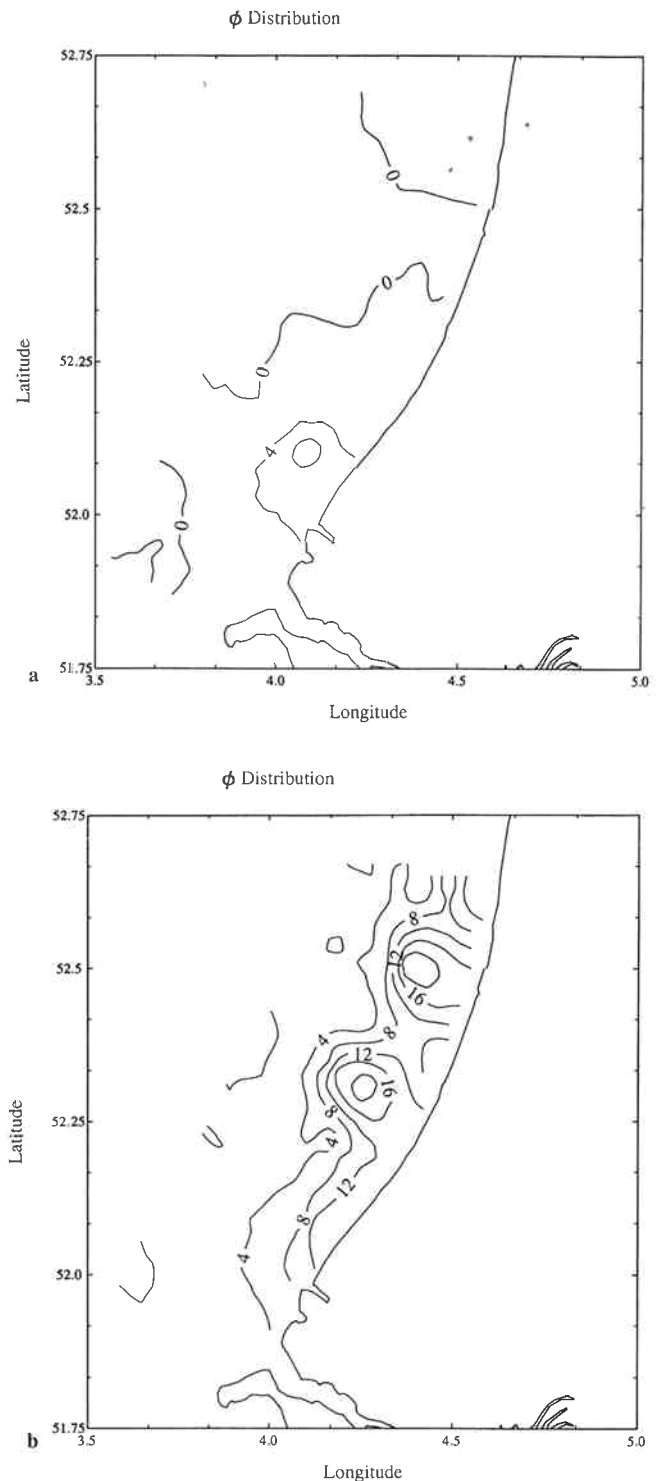


Figure 5

Distribution of potential energy anomaly ϕ in Jm^{-3} ; a) post-springs (8 to 10 October 1990); b) post-neaps (14 to 16 October 1990).

ture in response to other factors *e. g.* changes in stirring and density driven circulation.

In spite of these caveats, the implication of the surveys is that the springs-neaps switching between mixed and stratified conditions observed in the time-series measurements was typical of changes over the whole ROFI area. The re-stratification which occurred between the two surveys represents a relaxation under gravity of the horizontal gradients observed in the strongly mixed situation. The nature

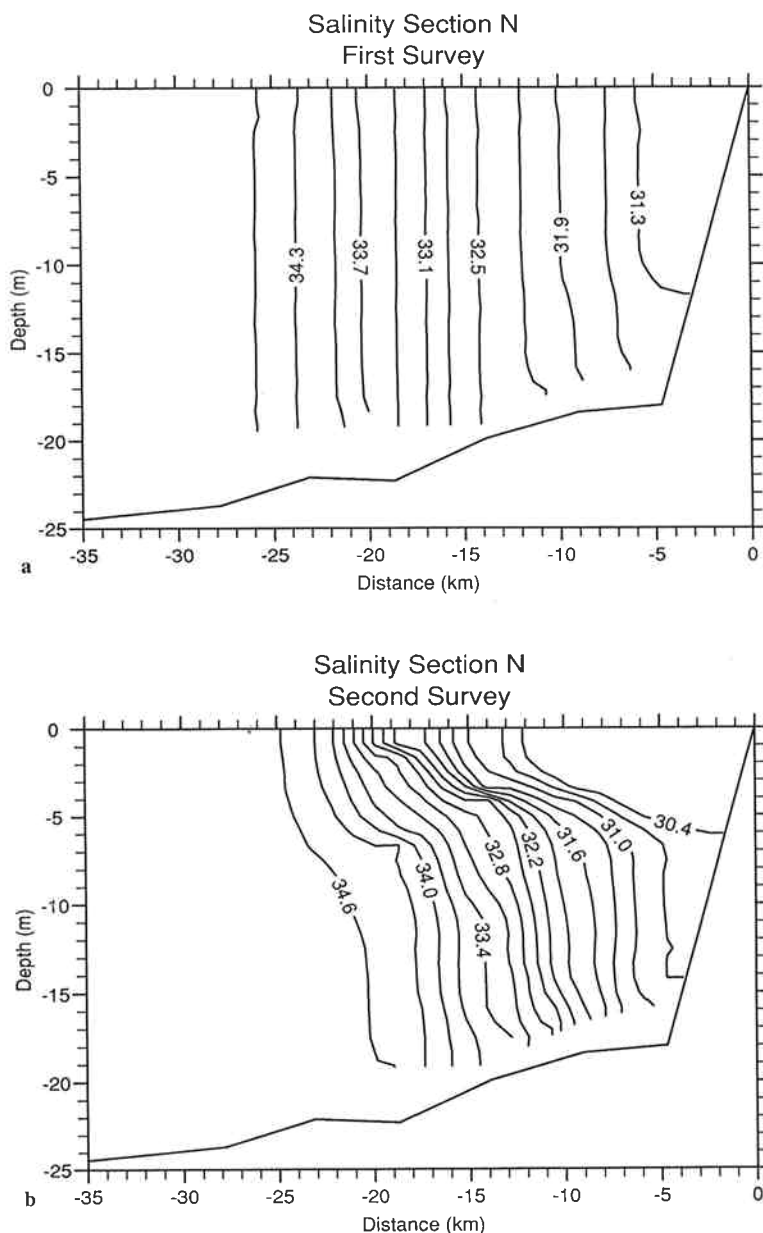


Figure 6

Salinity section on the N section (see Fig. 3). a) post-springs 9 October 1990; b) post-neaps 15 October 1990.

and the density and its gradients are mainly determined by the salinity distribution. Water with a salinity deficit of up to 4 is seen lying along the coast; most of the gradients are normal to the shore with only rather weak changes parallel to the coast (Fig. 7 a).

The observed nitrate distribution (Fig. 7 c) closely mimics the salinity field with high values up to 34 μM near the Rhine source decreasing to low levels offshore. A regression of nitrate on salinity shows a high degree of inverse correlation with $R^2 = 0.78$ (d.f. = 36) indicating the predominance of the Rhine as the nutrient source.

The flow field

The residual flow over the 16 day period of the CODAR observations is superimposed on the salinity plot of Figure 7 a. In the low salinity region close to the coast, the codar results indicate a coherent residual flow to the north which is approximately coast-parallel and has a typical speed of 15–20 cm s^{-1} . This flow extends out to the 34 isohaline after which the current decreases to much weaker values.

Near surface residuals determined by Rijkwaterstaat currentmeters on the M section for the same period also indicate net northward flow at a depth of 4 m but with rather lower speeds (5–15 cm s^{-1}).

Figure 8 shows fifteen days of wind, bottom-surface salinity difference and residual currents for the station 3 km from the coast on the M section. At the start of the time series, the water column is mixed and there is a strong correlation between the near-surface and near-bottom residual currents. With the onset of stratification about six days later, the bottom residual current is largely decoupled from the surface flow.

The change in coupling between surface and bottom currents is also indicated by a regression analysis of the wind-current response in the form:

$$V_y = aW_y + b$$

where V_y is the along-shore current and W_y is the along-shore wind. The regression analysis was carried out for two different periods; the first one was for a four day period when there was a strong wind event and the water column was mixed almost everywhere and the second one covered the whole span of the observations. A sample of the filtered wind and current data from the two period is plotted in Figure 9.

In the first (mixed) case, the analysis indicated that both surface and bottom residual currents were highly coherent

of this adjustment can be seen clearly in the plots of Figure 6 which show the contrasting salinity distributions on the Noordwijk (N) section. When vertical mixing is reduced, the pressure gradients due to the horizontal density gradients of Figure 6 a initiate a cross-shore flow like that in the laboratory experiments of Linden and Simpson (1988). The motion is, however, constrained by the earth's rotation and the cross-shore movement is limited to a length of order of the Rossby radius as can be seen in the neaps survey of Figure 6 b. The initial offshore flow is deflected into an alongshore coastal current in which the transverse pressure gradients are, to first order, balanced by the Coriolis forces. The observed adjustment is in fair accord with the two-layer gradient model of Ou (1983) which indicates a displacement of the isopycnals of the order of 1.5 Rossby radii or about 5 km as observed (Fig. 6).

Surface temperature, salinity and nitrate fields from the post-neaps survey are illustrated in Figure 7. Because of the high degree of vertical uniformity at this time, these surface values are close to water column averages. Here, as in the previous survey, temperature variation is rather small

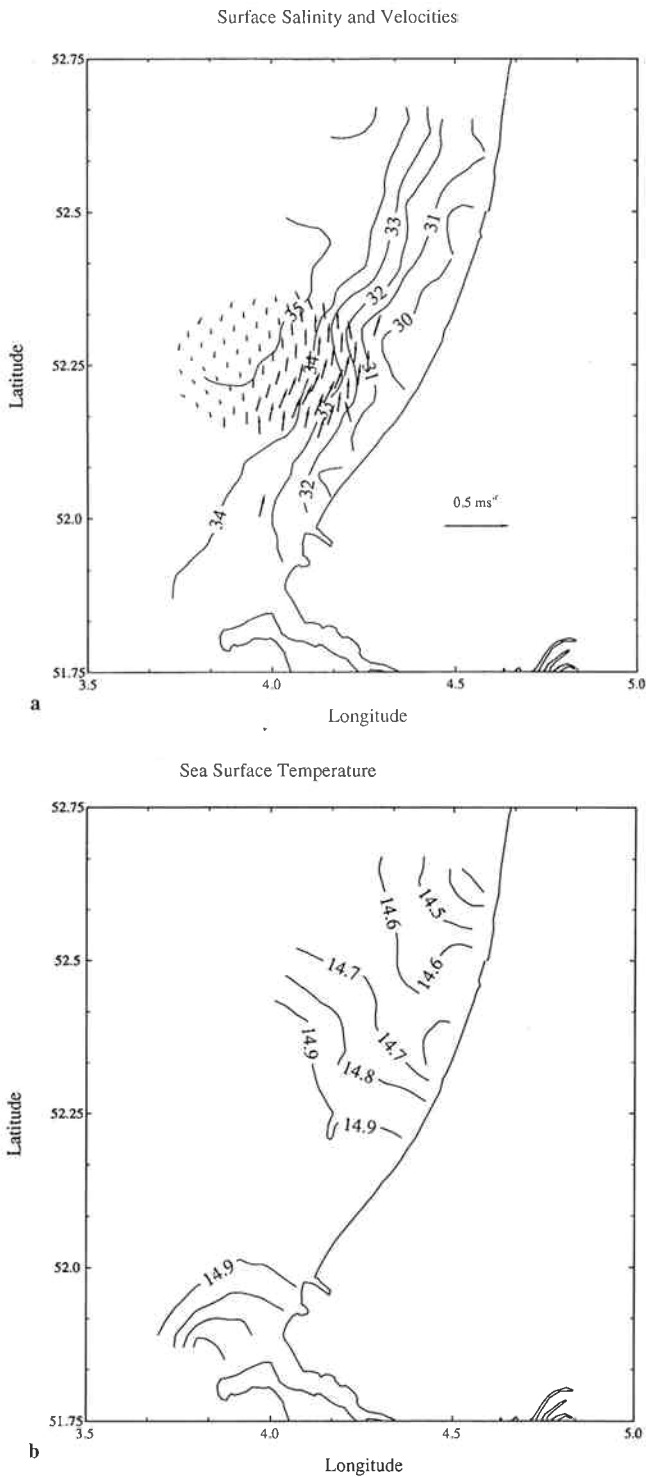


Figure 7

Surface distribution for the post-neaps survey (14 to 16 October 1990). a) surface salinity with mean surface velocities from CODAR; b) sea-surface temperature; c) nitrate in μM and near surface velocities from currentmeters.

SPM concentrations

Spatial distributions of suspended particulate matter (SPM) concentrations were determined from the CTD-deployed beam transmissometer using the calibration equation:

$$\Sigma = 3.44 (c - 0.479)$$

where Σ is SPM concentration and c is beam attenuation. The constants were established by fitting data from gravimetrically determined SPM concentrations of 100 bottle samples taken during the two surveys and over tidal cycles ($R^2 = 0.61$)

The contrasts in bottom resuspension, vertical mixing and water column structure between the two spatial surveys resulted in an equally marked contrast in SPM concentrations (Fig. 10). With the bottom stirring and vertical mixing that characterised the post-springs survey, SPM concentrations were high with typical values of 40-60 mg l⁻¹ in the near coast region (Fig. 10 a). A week later, surface concentrations had fallen by an order of magnitude (to 4-6 mg l⁻¹) in the stratified area to the north of the Rhine mouth, though values remained relatively high (in excess of 15 mg l⁻¹) in the mixed area of the mouth itself (Fig. 10 b). Furthermore, since the shore-normal gradients of turbidity and salinity were closely correlated during the neap period, advection of a front along these gradients was occurring at that time in the vicinity of the moorings thus producing the SPM peaks in the moored time series.

with the wind (R^2 of order 0.85) and gave a current/wind response factor of a ~ 0.01 .

For the full observation period, the response factors are similar but the coherence of the surface current with the wind is reduced with $R^2 = 0.7$ at 3 km off the coast and decreasing with distance from shore to $R^2 \sim 0.2$ at 33 km.

Examining the response times of the currents to the wind, it appears that, during springs, the along shore component of the current reacts in the order of half an hour. The cross-shore current-wind response is less strong because of the presence of the shore as a boundary. The strongest correlation was found at a time lag of 1.5 hour near the coast and of 3 hours at 33 km offshore.

Figure 8

Time series 3 km from the coast from 3 to 18 October 1992. a) wind vector at Noordwijk 10 m above the ground; b) salinity difference between 5 and 9 m deep; c) near surface and near bottom residuals at 4 and 12 m deep. Both wind and current have been rotated clockwise through 39.5° , so that the vectors lie parallel and perpendicular to the coast, as indicated in panel c.

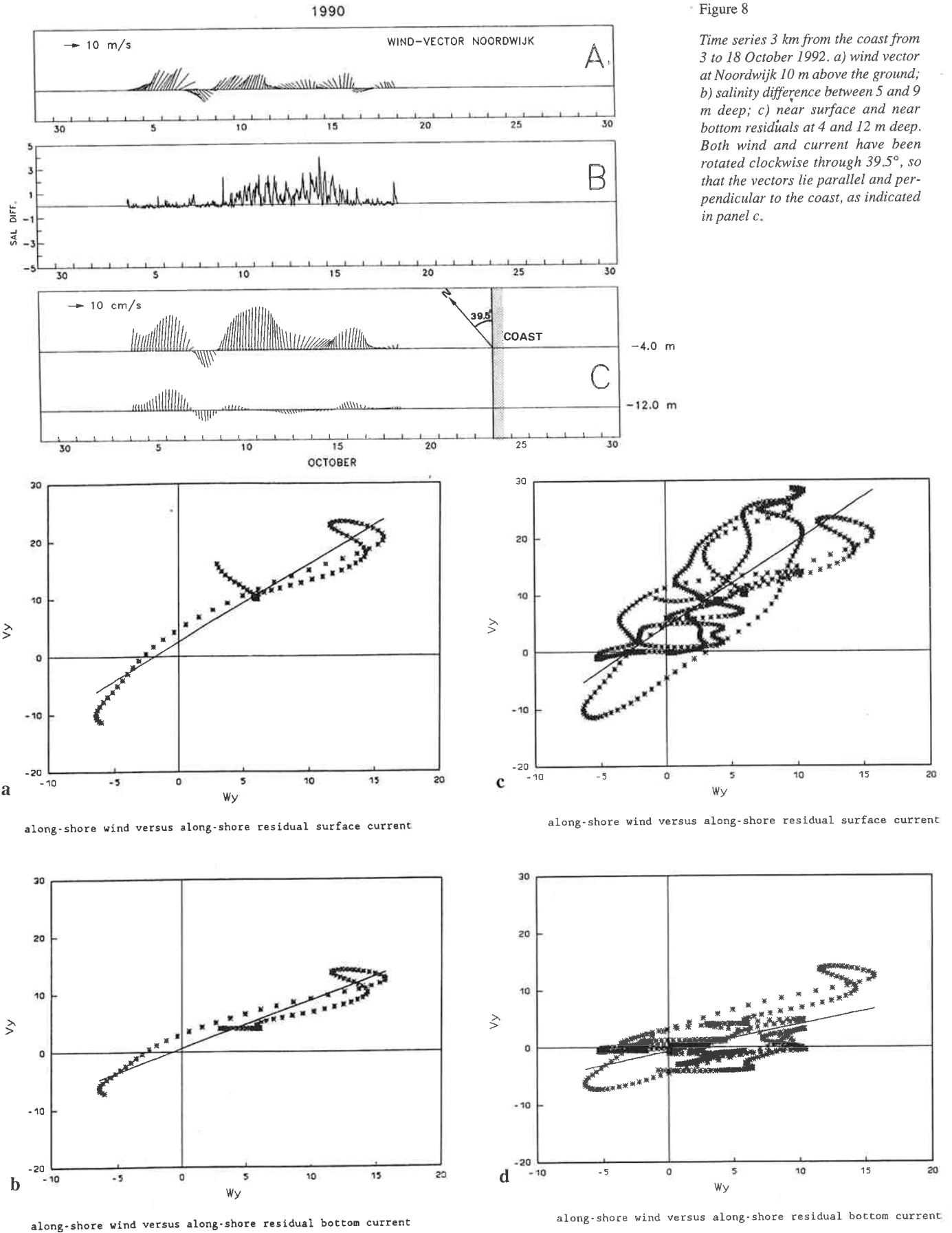


Figure 9

Alongshore components of current and wind. a) 4-8 October, near-surface current meter 3 km from the shore, 3 m deep; b) 4-8 October, near-bottom current meter 3 km from the shore, 12 m deep; c) 2-25 October near-surface current meter 3 km from the shore, 3 m deep; d) 2-25 October, near-bottom current meter 3 km from the shore, 12 m deep.

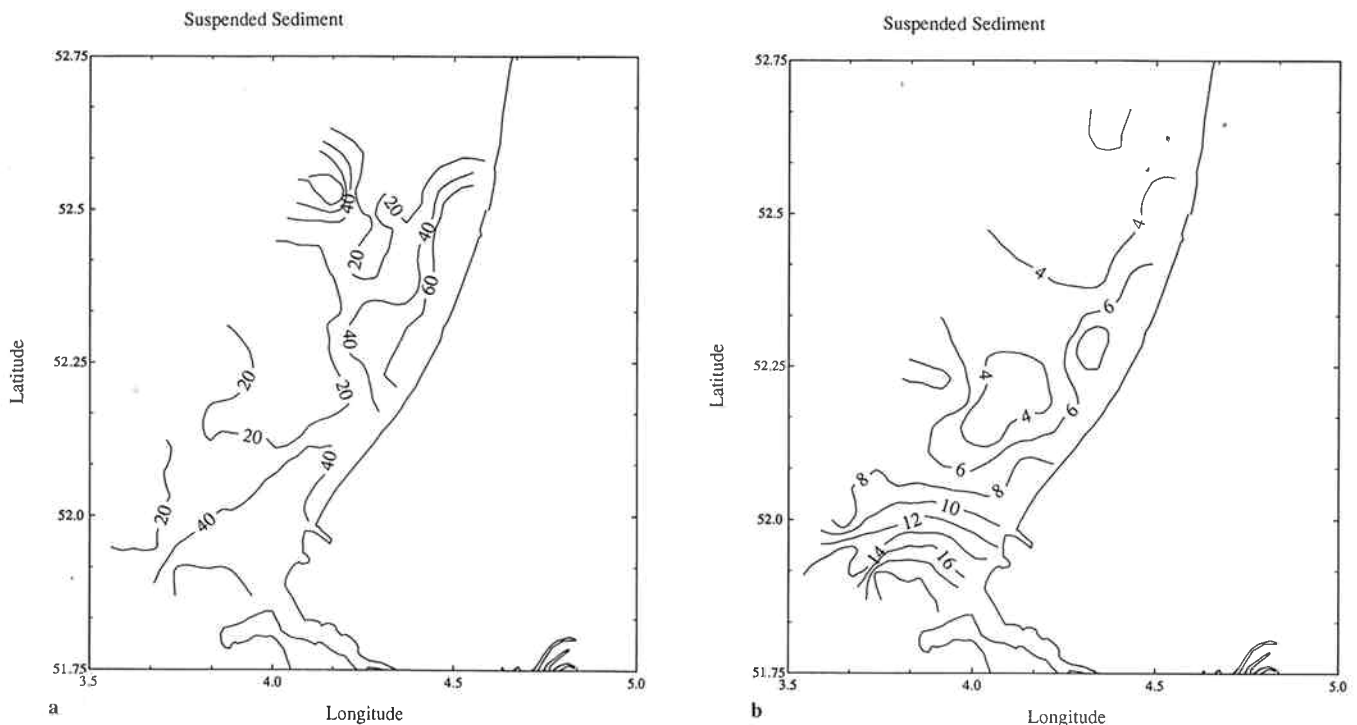


Figure 10

Surface total seston in mg l^{-1} . a) post-springs (8 to 10 October 1990); b) post-neaps (14 to 16 October 1990).

DISCUSSION

These new observations of the Rhine outflow region confirm the existence of a ROFI regime extending northwards along the Dutch coast from the Rhine source and out to approximately 30 km from the coast. Within this region, there is a residual northward flow and a vertical structure regime controlled by a competition between the stratifying influence of the freshwater outflow and stirring processes. The observed switching between stratified and mixed conditions occurred on the time scale of the springs-neaps cycle in accord with behaviour observed in other ROFI systems (Simpson *et al.*, 1990) but the fortuitous co-variance of wind and tidal stirring in this relatively short data set does not permit an unambiguous separation of their contributions.

The situation in this particular ROFI is also complicated by the exposed nature of the coast which allows long swell waves from storms in the northern North Sea and Atlantic to contribute significant forcing of turbulent mixing in the shallow water. This form of mixing was almost certainly making a significant contribution during the period days 276-281 when large swells from the northwest were incident on the coast.

Another mechanism, additional to those considered in our previous models of ROFI systems, is the dynamical influence of windstress at the surface. According to Münchow and Garvine (1992) the development of stratification is favoured by upwelling favourable winds and diminished by windstress in the opposite direction.

A striking feature of the time series observations is the very large semi-diurnal variability in stratification; this semi-diurnal stratification is considerably larger than that

observed in previous ROFI studies. Tidal straining (Simpson *et al.*, 1990) is probably primarily responsible for this large semi-diurnal signal but when, as in the present case, we are close to the Rhine source, enhanced semi-diurnal fluctuations may result from tidal displacement of the Rhine plume and the pulsed nature of the discharge. The occurrence of short periods of complete mixing on day 287 (Fig. 4), for example, suggests that the displacement to the northeast has brought unstratified water from the southwest to briefly occupy the mooring position.

The reduction of seston concentrations following the fall in stirring power is to some degree a characteristic of the whole coastal boundary layer. Our observations, however point to the additional effect of the ROFI regime in accelerating the drop in seston. The mechanism responsible would appear to be the onset of stratification which inhibits vertical mixing and thus facilitates the settling out of water column suspensions.

As well as providing a clearer picture of the operation of physical processes in the Rhine ROFI regime, this study has established an extensive data base, soon to be supplemented by further similar observations, for the testing and validation of high resolution models of the ROFI system which are being developed by MAST Profile programme.

Acknowledgements

This project was supported by the EEC through the MAST program under the MAST-0050C contract. A.J. Souza wishes to thank Conacyt, Mexico for the studentship provided. The authors would also like to thank R. Durazo for his valuable help with Uniras and to S. Boudjelas for the translation of the abstract.